Submitted to Nuclear Physics

LBL-689
Preprint

SECOND ORDER EFFECTS IN THE (h, t) REACTION

R. Schaeffer and N.K. Glendenning

May 1972

AEC Contract No. W-7405-eng-48

For Reference

Not to be taken from this room

LBL-689

DISCLAIMER

This document was prepared as an account of work sponsored by the United States Government. While this document is believed to contain correct information, neither the United States Government nor any agency thereof, nor the Regents of the University of California, nor any of their employees, makes any warranty, express or implied, or assumes any legal responsibility for the accuracy, completeness, or usefulness of any information, apparatus, product, or process disclosed, or represents that its use would not infringe privately owned rights. Reference herein to any specific commercial product, process, or service by its trade name, trademark, manufacturer, or otherwise, does not necessarily constitute or imply its endorsement, recommendation, or favoring by the United States Government or any agency thereof, or the Regents of the University of California. The views and opinions of authors expressed herein do not necessarily state or reflect those of the United States Government or any agency thereof or the Regents of the University of California.

0 0 0 0 3 7 0 7 3 2 9

LBL-689

To be submitted for publication in
"Nuclear Physics A"

May 1972
DPh-T/72/31

SECOND ORDER EFFECTS IN THE (h,t) REACTION*

by

R. SCHAEFFER† and N.K. GLENDENNING

Lawrence Radiation Laboratory
University of California, Berkeley, California 94720

*Work performed under the auspices of the U. S. Atomic Energy Commission.

†Present and permanent address :
CEN-Saclay, Service de Physique Théorique,
91, Gif-sur-Yvette, France

ABSTRACT

The excitation of the 2^+ analogues of the Cu isotopes of the lowest collective 2^+ states in the Ni isotopes through the reaction Ni(h,t)Cu is a case where the DWBA has to be corrected by two-step processes due to inelastic scattering in the initial and final states. The study of the interferences between first and second order terms shows that, in order to reproduce the experimental results, the effective interaction between the projectile and a bound nucleon has to be taken complex and not real, as is commonly assumed in the microscopic theory of inelastic scattering and charge exchange of helions and tritons.

I. INTRODUCTION

Due to recent experimental progress, the theory of the(h,t) reaction has been considerably improved. The early macroscopic[1] or microscopic[2] models have both been refined. From the optical parameters obtained by fitting elastic scattering it was realized[1,3] that, for both inelastic h scattering and charge exchange, the excitations should occur through the dominant imaginary coupling potential. On the other hand, the microscopic model[2] assumes generally real form factors, since the two-body nucleon-nucleon interaction is usually treated to first order. The microscopic, although totally phenomenological, theory of the (h,t) reaction is however in quite good shape. The strength of the effective force is typical[4,6] for each angular momentum transfer, and provided a tensor force[5,6] is used for unnatural parity transition, the experimental angular distributions can in general be reproduced quite well. There are however a few discrepancies. The most striking are the shapes of some $0^+ \rightarrow 0^+$ transition[7] which have an $L=1$ diffractional pattern due to the formation[27] of an intermediate α cluster and also the angular distributions for some 2^+ states[8,9] which have[8,9] minima and maxima greatly shifted from the expected DWBA predictions. These[8,9] anomalous 2^+ states are analogues of excited states of the target nucleus. We shall be interested in the study of these states for the Ni isotopes (and their analogues in the Cu isotopes) since in this case, very complete microscopic wave functions[10] are available. Moreover, the isospin structure of these states, which is very important for our study, could be deduced[11] from experiment (comparing (p,p') and (e,e') scattering). As explained below, this results in a strong inhibition of the direct (h,t) transition to the excited analogue in Cu (computed in the usual DWBA) compared to the (h,h') transition to the corresponding (collective) state in Ni. Therefore although two-step processes due to inelastic effects are generally seen to be negligible*, in this case the (h,h') excitation of the 2^+ lowest collective states in Ni followed by the (h,t) transition to its analogue in Cu can be expected to be very important. Both of these steps correspond to strong transitions whereas the usual one-step excitation is quite weak.

---

* Other two-step processes via more complicated states than the collective vibrational levels of the target nucleus cannot be excluded a priori. Both h and t projectiles break easily. The prediction of a complex form factor by the vibrational model can also be an indication that other higher order effects occur.

We shall use a microscopic formalism, in order to calculate the cross section for the (h,h') scattering to the collective states of the Ni isotopes and the (h,t) cross-sections to their analogues in the Cu isotopes : the first aim of nuclear reactions is to provide some information about the structure of nuclei. This is of course also achieved by the vibrational model which in this case provides[8] two deformation parameters $\beta^{(0)}$ and $\beta^{(1)}$. There is however no direct connection between these parameters and the microscopic wave functions of the states involved. The only way to get some precise information on the accuracy of these wave functions, is to use a microscopic description for the various transitions. For elastic scattering, however, we have still to rely on phenomenological optical potentials since there is yet no good microscopic theory in this case. Furthermore, since all reaction processes have to be included explicitly in a microscopic treatment of (h,h') and (h,t), it is possible to learn something about the various reaction mechanisms which lead to these transitions.

We shall investigate in detail the following points : i) is the DWBA transition to the analogue of the excited 2^+ state inhibited as suggested by the wave functions obtained by analysing (p,p') and (e,e') scattering ? , and ii) if yes, are two-step processes important and how do they change the cross-section ?

First, we have however to develop a suitable formalism which will permit us to carry on our study.

II. FORMALISM

1. The coupled equations

Provided an additional isospin quantum number is introduced, the set of coupled equations to solve for (h,h') and (h,t) scattering can be directly deduced from Ref.[12] .

$$\left(T_{c'} + V^{I}_{c'c'}(r) - E_{c'}\right) U_{c} = - \sum_{c''\neq c'} V^{I}_{c'c''}\, U_{c''}(r) \quad , \qquad (1)$$

$V^{I}_{c'c''}$ is related to the interaction $V(r,A)$ of the A+1 nucleus by

$$V^{I}_{c'c''}(r) = \langle \Phi_{c'\ I}(r,A) \,|V(r,A)|\, \Phi_{c''\ I}(r,A) \rangle \quad . \qquad (2)$$

The general philosophy of DWBA is i) to consider elastic transitions as strong and therefore to sum them up to all orders : $V^{I}_{c'c'}(r)$ is replaced by an optical potential $V^{(opt)}_{c'}(r)$ whose channel dependences reflect the two kinds of particles which are present in our problem and ii) to consider inelastic transitions as weak enough to be treated to first order. For the four channel problem we are interested in, the DWBA equations are therefore (denoting G and E the ground and excited states in the target, and A and AE their analogues) :

$$\begin{aligned}
\left(T + V^{(opt)}_{G}(r) - E_G\right) U_G(r) &= 0 \\
\left(T + V^{(opt)}_{E}(r) - E_E\right) U_E(r) &= V^{I}_{E,G}(r)\, U_G(r) \\
\left(T + V^{(opt)}_{A}(r) - E_A\right) U_A(r) &= V^{I}_{A,G}(r)\, U_G(r) \\
\left(T + V^{(opt)}_{AE}(r) - E_{AE}\right) U_{AE}(r) &= V^{I}_{AE,G}(r)\, U_G(r)
\end{aligned} \tag{3}$$

which represents equation (1) solved to the first order of the inelastic (or charge exchange) coupling, as shown in Fig.1a .

Whereas the couplings $V_{E,G}$ and $V_{A,G}$ are strong, $V_{AE,G}$ is expected to be weak and the last equation may have to be corrected for second order effects which might be of the same magnitude as the first order : the equation to solve in this case are therefore (Fig.1b).

$$\begin{aligned}
\left(T + V^{(opt)}_{G}(r) - E_G\right) U_G(r) &= 0 \\
\left(T + V^{(opt)}_{E}(r) - E_E\right) U_E(r) &= V^{I}_{E,G}(r)\, U_G(r) \\
\left(T + V^{(opt)}_{A}(r) - E_A\right) U_A(r) &= V^{I}_{A,G}(r)\, U_G(r) \\
\left(T + V^{(opt)}_{AE} - E_{AE}\right) U_{AE}(r) &= V^{I}_{AE,G} U_G(r) + V^{I}_{AE,E}(r) U_E(r) + V^{I}_{AE,A}(r) U_A(r)
\end{aligned} \tag{4}$$

This correction to Eq.(4) is expected to be important since $V_{AE,E} \sim V_{A,G}$ and $V_{AE,A} \sim V_{E,G}$: the two second order coupling potentials are therefore much stronger than the first order coupling.

The equations (4) have been solved using the source technique of Ascuitto and Glendenning[13]. They have the great advantage over the usual set of coupled equations, solved to all orders, of permitting the use of the usual

optical potentials without correction for double counting of some processes (as $G \to E \to G$).

2. Coupling Potentials and Transition Densities

a) Elastic Scattering

As usual, we have chosen $V_G^{(opt)}(r) = V_E^{(opt)}(r)$ as being the optical potential fitting the elastic scattering of ^{3}He particles at the energy E_G. Similarly, we have taken $V_A^{(opt)}(r) = V_{AE}^{(opt)}(r)$ to be the optical potential for elastically scattered tritons at an energy close to E_A. The significant difference between the helium and triton parameters is the radius of the imaginary part, which is[14,15] considerably smaller for tritons, reflecting[14,15] the smaller radius (due to the Coubomb effects) of the latter projectile. The potentials $V^I_{AG}(r)$ and $V^I_{AE,E}(r)$ can be deduced from this difference if one assumes isospin invariance. It is however not yet clear how good this assumption is, since the relevant part of the symmetry potential obtained this way is purely imaginary and arises from the different absorption radii for helium and tritons. As said above this difference arises at least in part from Coulomb effects in the projectiles and therefore should not be included in the symmetry potential. Anyway, consistent with the description of the inelastic or quasi-inelastic transitions, we have to use a microscopic model for V_{AE} and $V_{AE,E}$.

b) Inelastic Scattering and Charge Exchange

Following Refs.[12] and [16]* the potential coupling channels C_1 and C_2 can be written in terms of the more usual form factor F and the transition densities δ:

$$V_{C_1C_2} = \sum_{LSJ,T} V_{ST}\, C^I_{LSJ}\, F^{\alpha_1\alpha_2}_{LSJ,T}(r) \tag{5}$$

$$F^{\alpha_1\alpha_2}_{LSJ,T}(r) = \int_0^\infty V_L(r,r')\, \delta^{\alpha_1\alpha_2}_{LSJ,T}(r')\, r'^2\, dr' \tag{6}$$

$$\delta^{\alpha_1\alpha_2}_{LSJ,T}(r) = 4\pi \sum_{a,b} S^{ab}_{J,T}(\alpha_1\alpha_2)\, \langle j_a \| Y_{LSJ} \| j_b \rangle\, U_a(r)\, U_b(r) \tag{7}$$

$$S^{ab}_{J,T}(\alpha_1\alpha_2) = \frac{\langle \alpha_1 \| [\beta^+_a\, \beta_b]^T_{JT} \| \alpha_2 \rangle}{\sqrt{2J+1}} \quad . \tag{8}$$

---

* The difference in notation between Refs.[12] and [16] is explained in Ref.[16], footnote p.60 .

The reduced matrix element is taken in the spin space only, but not in the isospin space.

The amplitude S relative to the Ni excited states and those relative to their analogues in Cu are closely related. The wave functions for the analogues are

$$|A\rangle = \frac{1}{\sqrt{N_A}} T_- |G\rangle \tag{9}$$

$$|AE\rangle = \frac{1}{\sqrt{N_{AE}}} T_- |E\rangle \tag{10}$$

We assume also that the states $|G\rangle$ and $|E\rangle$ have a good isospin T_o. This is a very good approximation[17] for the ground state. For the excited state, the isospin violating terms are built of particles excited from orbitals occupied by both neutrons and protons to orbitals with neither protons nor neutrons, which play only a small role in the usual models.

Moreover, these models still overestimate[17] this admixture. The approximation of good isospin can therefore be expected to be very good. If T_o is the isospin of the states considered, $N_A = N_{AE} = 2T_o$ and

$$\begin{aligned} T_+ |G\rangle &= 0 \\ T_+ |E\rangle &= 0 \end{aligned} \tag{11}$$

The amplitude S for the transition $G \to AE$ is :

$$S^{ab}_{J,T}(AE,G) = \frac{\langle AE \| [\beta^+_a \beta_b]^{-1}_{JT} \| G\rangle}{\sqrt{2J+1}} \tag{12}$$

Using (10) and (11) and the standard[18] commutation rules of isospin operators, S can be expressed as

$$S^{ab}_{J,T}(AE,G) = \frac{\delta_{T1}}{\sqrt{T_o}} \frac{\langle E \| [\beta^+_a \beta_b]^{O}_{J1} \| G\rangle}{\sqrt{2J+1}} = \frac{\delta_{T1}}{\sqrt{T_o}} S^{ab}_{O,T}(E,G) \tag{13}$$

Similarly, for the transitions $G \to A$ and $E \to AE$, we get, for zero spin transfer

$$S^{ab}_{O,T}(A,G) = \frac{\delta_{T1}}{\sqrt{T_1}} \langle G \| [\beta^+_a \beta_b]^{O}_{O,1} \| G\rangle = \delta_{T1}\, \delta_{ab} \frac{n_a^{(n)} - n_a^{(p)}}{\sqrt{2T_o}} \tag{14}$$

$$S^{ab}_{0,T}(AE,E) = \frac{\delta_{T1}}{\sqrt{T_o}} \langle E \| [\beta^+_a \beta_b]^0_{0,1} \| E \rangle = \delta_{T1} \delta_{ab} \frac{n_a^{(n)} - n_a^{(p)}}{\sqrt{2T_o}} \qquad (15)$$

$n_a^{(x)}$ is the occupation probability of shell a by neutrons $(x=n)$ or protons $(x=p)$ in the target ground state. Strictly speaking, the probabilities used in Eq.(15) should be taken for the target excited state E . The approximation involved by the use of (15) is exactly the same as the one made by replacing the optical potential in the channel E by the potential fitting elastic scattering in the channel G . Similarly, the amplitudes $S^{ab}_{J,T}(AE,E)$ for $J \neq 0$ should be omitted for consistency with the approximations* made for the elastic channels. Anyway, these amplitudes do not add coherently for $J \neq 0$ when summed over a or b , whereas they do for $J=0$. The assumption $S^{ab}_{J\neq 0,T}(AE,E) \approx 0$ is therefore not very important for the calculation we have made.

c) Transition Densities

The advantage of introducing the form factors and transition densities is that, for each transition we consider, there is almost only one set (LSJ,T) for which F or δ are sizeable. Since the G and A are 0^+ states, only one value of the spin transfer J is allowed for the $G \to A$, $G \to E$ and $A \to AE$ excitations. This is also true for the transition $E \to AE$ within the approximation $J \sim 0$ discussed earlier.

The quantum numbers L ($L=J$ since we are dealing with natural parity states) and J can therefore be included in the labels α_1 and α_2 . The transition density (7) can therefore be denoted more simply $\delta^{\alpha_1 \alpha_2}_{ST}(r)$.

We shall make some further approximations, which will not be used in the actual calculations, but will provide some physical insight into the mechanism of collective excitations.

From (7) one can see that δ_{ST} is a coherent sum of densities describing the transition $a \to b$ with some spin transfer S and isospin transfer T

$$\delta^{\alpha_1 \alpha_2}_{ST}(r) = \sum_{ab} \delta^{\alpha_1 \alpha_2}_{ST,ab}(r) \qquad . \qquad (16)$$

---

* In principle a momentum transfer $J \neq 0$ is allowed for elastic scattering on a state with non-zero spin. Assuming that the optical potential is the same for excited states (with non zero spin) as for the ground state (with zero spin) amounts to neglect all $J \neq 0$ transfers in elastic scattering.

Equivalently, one could have considered the densities relative to proton or neutron excitations :

$$\delta_{Sp}^{\alpha_1\alpha_2}(r) = \frac{\delta_{SO}(r) - \delta_{S1}(r)}{\sqrt{2}}$$
$$\delta_{Sn}^{\alpha_1\alpha_2}(r) = \frac{\delta_{SO}(r) + \delta_{S1}(r)}{\sqrt{2}} \qquad (17)$$

Formulae (5) and (6) could also have been written in terms of proton and neutron excitations, V_{ST} being replaced by V_{Sp} and V_{Sn} .

All nuclear models for collective states predict the sum (16) to be small for $S=1$. This can be understood[17,18] since V_{1p} and V_{1n} are repulsive and V_{Op} , V_{On} are attractive for any reasonable nucleon-nucleon force. Therefore the collective states are those which possess the particular correlations that are induced by the attractive part of the force and are, so to speak, anticollective with respect to the repulsive parts. This is only possible since the sum over a and b runs over a sufficient number of orbitals with different spin orientations (that is $j = \ell+1/2$ and $j = \ell-1/2$ in j-j coupling).

In isospin space, since V_{OO} is attractive and V_{O1} repulsive, the same argument can be used, leading to the prediction $\delta_{O1} << \delta_{OO}$. However in the current nuclear models, the possible $a \rightarrow b$ excitations are generally sufficiently different so these models do not predict the averaging out of the $\delta_{O1}(r)$ transition densities. For the nuclei we are considering, the Ni isotopes, the proton shell is closed and the neutron shell is open. For these reasons many models[20] consider the lowest (collective) 2^+ state as built only out of neutron excitations, that is

$$\delta_{O1}(r) = -\delta_{OO}(r) \qquad . \qquad (18)$$

More realistic models[10], which include excitations of both kinds of particles lead[10,11,19] to the approximate relations

$$\delta_{O1}(r) \approx -\frac{1}{2}\,\delta_{OO}(r) \qquad (19)$$

for the 2^+ collective state. The proton excitations (obtained using Eq.(17)) which are inhibited by the gap associated with the closed shell, are still about 3 times less important than neutron excitations. Within the same model[10], the 3^- collective state for which both proton and neutron shells behave almost as closed, leads to the relation

$$\delta_{01}(r) \approx -\frac{1}{5}\,\delta_{00}(r) \quad . \tag{20}$$

Finally, the ratio of proton and neutron excitations, as extracted from experiment by comparing (p,p') and (e,e') scattering using the method of Refs. [11] and [19], leads to $T=1$ transition densities at least 10 times smaller than the $T=0$ ones.

This has an important consequence in comparing (h,h') and (h,t) cross-sections relative respectively to the E and the EA states. From (13) it follows that the $G \to EA$ transition goes through $\delta_{01}(r)$ whereas the $G \to E$ transition is dominated by $\delta_{00}(r)$, the contribution of $\delta_{01}(r)$ being small (this is true even if δ_{01} is not much smaller than δ_{00}, since $V_{01} \ll V_{00}$ for the mass 3 particles we consider). The comparison of the E and EA cross-section strengths leads therefore to a direct determination of the ratio of the $T=1$ versus the $T=0$ excitations. From the results obtained [11,19] by comparing (p,p') and (e,e') experiments, one can expect the $G \to EA$ transition to be strongly inhibited compared to the $G \to E$ transition.

III. DIRECT TRANSITIONS (THE USUAL DWBA)

In order to compare the transition densities (7) for proton and neutron excitations, we have calculated the Ni(h,t)Cu cross-sections for the first 2^+ excited analogue which were measured by Kunz et al. [8]. We have used the wave functions of Gillet et al. [10], which are the most realistic, corrected in the same way as in Refs. [11] and [19]. We shall briefly recall the method used for this correction.

1. Model Wave Functions and Real Transitions

Gillet, Giraud and Rho describe [10] the ground state of the Ni isotope as a proton closed shell and a neutron BCS state. In this model, the lowest 2^+ excited state of Ni is a mixture of a large number of particle-hole proton and two quasi-particle neutron states. The transition densities (labelled $\delta^{\alpha_1\alpha_2}_{s,x}(r)$, $x = p$ or n) present therefore a collective behavior for both proton and neutron excitation, that is are peaked at the nuclear surface. One can therefore expect the true densities δ to be proportional to the model ones :

$$\delta_{s,p}^{\alpha_1\alpha_2}(r) \approx \lambda_p \, d_{s,p}^{\alpha_1\alpha_2}(r) \tag{21}$$

$$\delta_{s,n}^{\alpha_1\alpha_2}(r) \approx \lambda_n \, d_{s,n}^{\alpha_1\alpha_2}(r) \tag{22}$$

In Refs. [11] and [19], λ_p was chosen in order to reproduce the experimental B(E2) value and λ_n then fitted in order to obtain the strength of the (pp') cross-section. Since the same densities (21) and (22) appear in the scattering amplitude of the (h,t) transition to the excited analogue, 2^+ state in Cu, it is possible to obtain another value of λ_n, independent of the (p,p') estimate, and therefore check the property shown in Refs. [11] and [19], i.e. $\delta_{0,p}^{\alpha_1\alpha_2}(r) \approx \delta_{0,n}^{\alpha_1\alpha_2}(r)$. Since the (h,t) amplitude is proportional to $\delta_{0,n}(r) - \delta_{0,p}(r)$ which almost cancel, a slight variation of λ_n produces a very large change in the (h,t) cross-section strength. The determination of λ_n by this method should therefore be quite precise.

An alternative way of obtaining the correction factors λ_n and λ_p would be to fit simultaneously the (h,h') cross-section to the Ni 2^+ collective state and the (h,t) cross-section to the Cu excited analogue. We have not used this method since there is only one inelastic He^3 experiment available[21] : $^{58}Ni(h,h')^{58}Cu$. In addition, this latter method requires the knowledge of the effective force for both (h,h') and (h,t) scattering and introduces therefore an additional uncertainty.

In order to characterize more simply the ratio of proton and neutron excitation, we introduce the quantity

$$\rho = \frac{\int_0^\infty r^2 \, \delta_{0,n}(r) \, r^2 \, dr}{\int_0^\infty r^2 \, \delta_{0,p}(r) \, r^2 \, dr} \tag{23}$$

as was done in Refs. [11] and [19]. The ratio ρ, as extracted from experiment, has the advantage of being easily calculable and provides a straightforward check for any nuclear model since it is directly related to the commonly used isoscalar and isovector electromagnetic transition rates.

2. Choice of Parameters

The optical potential parameters are taken from Ref. [8], where it was noticed that different parameters for the h and t channels lead to slightly

better fits. We have therefore used the parameters of Table 1 .

The effective projectile-target nucleon interaction for (h,t) is quite well known[4,5]. We assume a Serber mixture for the nucleon-nucleon potential, and deduce the (h,t) mixture parameters in the usual[2] manner. The choice of the force mixture is not important in this case since there is almost only one force parameter contributing to the scattering amplitude ; $V_{S=0\ T=1}$, for the collective, natural parity state we consider. The strength of the effective (h,t) force was fitted in order to reproduce on the average the experimental strength of the $G \rightarrow A$ transition, for the various isotopes.

We have therefore used the following parameters :

$$V_{01} = V_{11} = 7.5 \text{ MeV} \qquad (24)$$

3. Results

a) $^{58}Ni(h,t)^{58}Cu$

Using the transition densities extracted[19] from (e,e') and (p,p'), the predicted cross-section for the 2^+ EA is about a factor 8 too low (Fig.2). However, a 30% change in λ_n leads to the right magnitude for this cross-section (Fig.2). Such a variation of λ_n is within the errors of the method used in Refs.[11] and [19] for its determination. The slight uncertainty in the parameters V_{01} and V_{11} does not lead to important changes in this value of λ_n .

The new value of λ_n corresponds to a ratio of neutron over proton excitations $\rho = 1.2$ compared to $\rho = 0.9$ for (p,p') (the ratio obtained with the wave functions of Ref.[10], that is without the correction factors λ_p and λ_n , is $\rho = 2.8$).

It is interesting to notice that the transition densities we obtain lead to a very good agreement for the $^{58}Ni(h,h')^{58}Ni$ cross-section to the 2^+ excited state (Fig.2). For the effective h-target nucleon inelastic interaction we have used a Serber mixture (as for the charge exchange reaction, this is not a very important assumption, since in this case practically only V_{00} contributes to the scattering amplitude). We have fitted the force strength in order to reproduce the $^{40}Ca(h,h')^{40}Ca$ $(3^-,3.74)$ cross-section with the wave functions of Gillet and Sanderson which are believed[23,24] to be quite good.

We have also examined the (h,t) cross-section when allowing larger variations of λ_n . From Fig.3, it can be seen that for $\lambda_n = 1.2$, the AE cross-

section almost vanishes. This corresponds to the cancellation of the tails of the proton and neutron transition densities, and to $\rho = 0.8$. As can be noticed the r^2 integrals of $\delta_{0,n}$ and $\delta_{0,p}$ cancel each other for a slightly different value of λ_n ($\lambda_n = 1.5$) , corresponding to $\rho = 1$. This is not astonishing since the strong absorption favors much more the tail of the transition density than the r^2 factor does.

Fitting the value of λ_n to the (h,t) cross-section leads actually to two values (Fig.3), corresponding to opposite signs for $\delta_{01}(r)$. The second value we obtain is $\lambda_n = 0.6$, that is $\rho = 0.3$. This value should however be rejected since it reproduces neither the (pp') nor the (h,h') cross-section strengths (Figs.2,3)

b) Other Ni isotopes

All the Ni isotopes (60,62,64) present very similar features, and the transition densities obtained by fitting the (h,t) cross-sections are consistent with those obtained from (pp') scattering (Table 2). Although the ratio of neutron over proton excitation is much closer to 1 than the theoretical prediction and confirms therefore the conclusions of Refs.[11,19] it is found to be systematically larger than when obtained from (p,p') and (e,e') scattering. This difference might be due either to the uncertainty in the parameters used here, or more probably reflect the assumption (21), that is that the renormalization is independent of r . Since we have used harmonic oscillation single particle wave function, λ_n may have to be larger for reactions with strong absorption which weight more the tail of the transition densities.

If the angular distribution calculated for the ^{58}Cu 2^+ EA was acceptable (Figs.2 and 4), those for the higher isotopes are not (Fig.4). Whereas the theoretical angular distributions all exhibit a typical diffraction pattern and are therefore quite similar, the experimental patterns present marked differences (Fig.4) for the 60 and 64 isotopes (and probably also for ^{62}Ni, but the lack of measurements in the interesting region around 20° make any precise conclusion difficult).

This discrepancy is not particular to the microscopic model, since it can also be noticed in the vibrational picture when a real form factor is used[8].

4. Conclusion

An important piece of information has been obtained for the Ni isotopes using the DWBA approximation : although proton and neutron shells are quite dif-

ferent, one being closed and the other open, for the lowest 2^+ collective state the strengths of the proton and neutron excitation are quite similar. This confirms the results obtained[11,19] from (p,p') and (e,e') scattering, but is not predicted by any nuclear model for these 2^+ states.

An equal strength for proton and neutron excitations leads however to a strong inhibitions of the first order DWBA transitions and therefore second order effects might be important. The discrepancy seen for the angular distributions may be due to such higher order processes.

IV. INDIRECT TRANSITIONS

Equation (6) provides an indirect excitation of the EA by means of two different processes (Fig.1b).

1) The inelastic (h,h') excitation of the collective E state followed by a charge transfer $E \rightarrow EA$. Among the collective states of the Ni target only one has to be considered, since the transition of an excited state to its analogue is much stronger than to any other state.

2) The charge exchange reaction to the analogue of the Ni ground state : $G \rightarrow A$ followed by an inelastic (t,t') excitation $A \rightarrow EA$ which is expected to be as strong as the collective $G \rightarrow E$ transition.

1. Parameters

The two new coupling terms in Eq.(4) are given by formulae (5) to (15). The effective projectile-target nucleon interaction for $V^I_{AE,E}$ is the same as for $V^I_{A,G}$ since both coupling terms describe a (h,t) transition with 0^+ spin and parity transfer. Similarly, the same force parameters can be used for $V^I_{AE,A}$ and $V^I_{E,G}$ after having corrected for the isospin dependence of the projectile. All the force constants are chosen to be real. This choice is crucial, since it determines the interference properties of first and second order contributions.

As said earlier, the vibrational prediction for the transition operator shows that the effective force to be used in the microscopic description might be complex. The evidence for such a feature is however difficult to obtain from a DWBA process ; even if the real and imaginary parts of the force have a different radial behavior, since the cross-section is sensitive to the modulus squared, it is quite possible to obtain good fits with a pure real interaction. A change

$e^{i\Phi}$ in the phase of the projectile-target nuclear multiplies the one-step contribution in Eq.(4) by $e^{i\Phi}$, and the two-step contribution by $e^{2i\Phi}$. It is therefore possible to get some information about the phase of the effective interaction by studying the interferences of one and two step processes.

The force we use (referred as force I) is therefore :

$$v(r) = (-28.5 + 7.5\tau_1\tau_2 + 7.5\sigma_1\sigma_2 + 7.5\sigma_1.\sigma_2.\tau_1.\tau_2)\, e^{-(\frac{r}{2.25})^2} .$$

The first two parameters V_{00} and V_{01} being fitted to experiment and the less important V_{10} and V_{11} being simply assumed to be equal to V_{01}.

The 7.5 MeV strength needed in order to fit the $G \rightarrow A$ cross-section can be compared to the 6 MeV needed[4] for the $^{48}Ca(0^+,G)\ ^{48}Sc(0^+,A)$ transition. Park and Satchler[15] use a much lower value, 2.5 MeV , but the (h,h') cross-sections they calculate are not very sensitive to this parameter. For V_{00}, they use 22.5 MeV which is deduced[15] from realistic forces. This value leads to slightly too low a cross-section for $^{40}Ca(0^+,8^-)$ around 40°, even when Saxon-Wood radial orbitals are used for the bound states (we use harmonic oscillator wave functions with the standard parameters $h\omega = 41\ A^{-1/3}$ MeV and therefore $b = 1.00\ A^{1/6}$ fm).

2. Real Effective Interaction

Using the transition densities fitted previously, one obtains quite a small second order contribution for the excitation of the $^{58}Cu,2^+$ EA . It increases however the cross-section by about 30%. The value of λ_n needed in order to reproduce the magnitude of the experimental $^{58}Ni(h,t)^{58}Cu$ cross-section after having taken the two-step process into account is only 10% smaller than the DWBA value. Nevertheless, including the two-step produces (Fig.4) a slightly better angular distribution because of an overall shift of about 2° towards smaller angles.

When λ_n is varied over a large scale, from 0.7 to 2 the DWBA cross-section at the maximum around 25° varies by almost two orders of magnitude (Fig.3). Nevertheless, the two-step contribution leads to almost a constant increase (about 4 μb), and can be therefore seen to contribute incoherently to the 2^+ EA cross-section.

For the other Ni isotopes, the two-step contribution is larger. This is not astonishing since the $G \rightarrow A$ (and therefore also the $E \rightarrow EA$) coupling

potential increases like $\sqrt{N-Z}$, whereas the $G \rightarrow E$ and $G \rightarrow AE$ amplitudes are roughly constant. Qualitatively, this is the effect observed experimentally : the discrepancy with the DWBA calculation is more important for the higher mass isotopes. But the washing out of the diffractional pattern, obtained when two-step processes are included, and which is characteristic of an incoherent contribution has little to do with the experimentally observed angular shifts.

We have nevertheless fitted new values of λ_n in order to obtain a better estimate of the neutron transition density (Fig.4 and Table 2).

An attempt to change the interference properties by using different optical parameters was unsuccessful. With any reasonable potential, i.e. fitting elastic h or t scattering at about the energy of the experiment, the first and second order contributions remain incoherent.

3. Complex Effective Interaction

Since the second order contribution to the scattering amplitude may interfer with the first order one, the resulting cross-section are expected to be quite sensitive to the relative phase of the two contributions to the scattering amplitude. This phase may arise from the interplay of the various partial waves, but, as seen earlier it is difficult to modify the interference properties by changing the optical potential. On the other hand, different interference properties can be easily obtained by using a complex nucleon-nucleon interaction. This may be justified by the contribution of higher order terms in the effective force.

However, if the introduction of a complex phase seems therefore likely, it is by no means obvious that such a phase

i) will produce any angular shift, and especially the right shift needed in order to reproduce the observed pattern.

ii) even if it produces the needed shift, will have a value consistent with the vibrational model.

We shall of course make quite a few simplifying assumptions. The usual, real force $\bar{v}(r)$ has a range of about the size of the projectile after averaging with the h or t wave functions. A complex nucleon-nucleon force $v(r) + iw(r)$ leads therefore to an effective interaction $\bar{v}(r) + i\bar{w}(r)$ where $\bar{v}$ and $\bar{w}$ have similar ranges even if v and w have not. If therefore the complex phase comes from the nucleon-nucleon interaction itself, it may be simulated by simply multiplying the usual force $\bar{v}(r)$ by $e^{i\Phi}$, Φ being a constant phase. We shall refer thereafter to the interaction $e^{i\Phi}\,\bar{v}(r)$ as force II . Of course, if the

complex phase arises from a process particular to the (h,h') and (h,t) reaction, $\bar{w}(r)$ may have quite a different range than $\bar{v}(r)$. It might even be non local. There is actually some evidence[4,25] that the variations as a function of the spin transfer of the effective force needed to fit the experiment cannot be reproduced by a local interaction. However, we have no indication a priori how $\bar{v}(r)$ should be modified. We shall therefore use force II as a first guess and make afterwards the changes in the force parameters that might be necessary in order to fit experiment.

a) Force II

There is no a priori limitation on the values that Φ might have, except $0 < \Phi < \frac{\pi}{2}$ if one wants to have a form factor with the same phase than for the macroscopic model.

A phase $\Phi = \frac{\pi}{4}$ leads already to a characteristic shift in the calculated angular distribution (Fig.5), the effect being larger for the isotopes with more neutron excess (the two-step contribution increases as $\sqrt{N-Z}$ whereas the direct contribution is roughly constant). It can also be noticed especially for ^{62}Ni and ^{64}Ni, that the slope of the calculated angular distribution is not steep enough, compared to experiment, when the indirect transitions are important. More interesting, however, is that the shift goes towards the smaller angles, that is the calculated pattern is much closer to the experimental one.

For $\Phi = \frac{\pi}{2}$, the effect is over emphasized (Fig.6), the angular distributions being shifted slightly too much, and the fall off being even slower.

A phase $\Phi = \pi$ leads, as for $\Phi = 0$, incoherent contributions from the direct and indirect amplitudes, and therefore it is not possible to obtain any shift in the angular distribution.

Although $\Phi = \frac{3\pi}{2}$ leads also to interferences between one and two-step processes, it was not possible to obtain a pattern bearing some resemblance with the experimental one (Fig.7).

The main conclusion of this calculation is that a complex phase $\Phi \approx \frac{\pi}{4}$ in the effective interaction is able to explain the shift of the maxima and the minima of the angular distribution when the two-step processes are included. The radial shape of the force, as deduced from the nucleon-nucleon interaction averaged over the projectile density, is however not able to reproduce the fall off of the experimental angular distribution. It is also interesting to notice that, although a complex phase brings important changes, the cross-sections vary rather smoothly with Φ, the results with $\Phi = \frac{\pi}{4}$ and $\Phi = \frac{\pi}{2}$ being qualitatively iden-

tical, although differing quantitatively. The range $\frac{\pi}{4} < \Phi < \frac{\pi}{2}$ seems to be acceptable and leads to maxima and minima at about the right angles.

b) Force III

To correct the fall off of the calculated angular distribution, we have simply increased the range of $\bar{v}(r)$. Since the previous calculation have shown that a complex interaction is needed, there is actually no reason for keeping the range deduced from the standard, first order calculation which anyway leads to only a real force. The best results were obtained with a range of 3 fm (that is an increase of about 30% compared to the usual values). A somewhat smaller range would probably better fit the (h,h') cross-sections at angles larger than 60°, but it was noticed earlier[4] that long range forces give quite acceptable fits to the (h,t) cross-sections at angles beyond 60°. In addition, increasing the range has the advantage (Figs.7,8) of shifting slightly the maxima in the right direction already for the one-step calculation. The strength of force III has been renormalized in order to obtain the same cross-sections to the analogue states as for force I and II (since we treat the indirect excitations to the lowest order in the coupling constant, the cross-section to the analogue is not affected by the inclusion of the two-step contribution).

Force III is therefore

$$v_{III}(r) = e^{i\Phi}[5.6 + 1.35(\sigma_1 . \sigma_2 + \tau_1 . \tau_2 + \sigma_1 . \sigma_2 . \tau_1 . \tau_2)]\, e^{-(\frac{r}{3})^2} .$$

As expected, $\Phi = \frac{\pi}{4}$ and $\Phi = \frac{\pi}{2}$ lead to quite good fits for the angular distribution after the two-step contribution has been included, the agreement being better for $\Phi = \frac{\pi}{2}$. As for force II, the direct transitions lead to the same angular distributions for all isotopes, and the indirect transitions are really needed in order to reproduce the increasing shift for the nuclei with the larger neutron excess (Fig.8).

Since the indirect transitions affect the magnitude of the EA cross-sections as well as their pattern, slight adjustments had to be made for the values of λ_n (λ_p being fixed to its (e,e') value). The new values for λ_n are given in Table 2 . As can be seen this parameter is somewhat sensitive to the choice of the complex phase for the interaction. Since we had to adjust quite a few parameters before being able to reproduce the EA cross-sections, we expect these values of λ_n not to be too precise. In particular, these values are found to be systematically larger than those obtained from (p,p') scattering.

Nevertheless, they display qualitatively the same feature as seen from (p,p') and (e,e') : the excitations of neutrons and protons have within a factor of 2 the same strength, although the proton shell is closed and the neutron shell open. It is interesting to note the increasing amount of neutron excitation with increasing neutron excess. A systematics of high energy (p,p') or (α,α') experiments would be the most accurate way to check this point.

To summarize, the following calculations have been made :

i) with a real interaction, the transition density is extracted[11,19] from (p,p') and (e,e') experiments, without any adjustable parameter. Within the uncertainties of the extraction[11,19], these transition densities lead to acceptable cross-section strengths for the 2^+ E state, excited by (h,h') and the 2^+ EA , excited by (h,t). Second order effects are already seen to be very important. The angular distributions are however poorly reproduced.

ii) with an adjustable complex phase for the potential, which is crucial for reproducing the experimental maxima and minima of the angular distribution by allowing interferences between direct and indirect transitions. An even better agreement with experiment can be obtained, provided an additional change in the force range corrects for the slope of the angular distribution.

V. CONCLUSION

We have examined the (h,t) transition which feeds the analogue of a collective 2^+ state of the target. This is a very favourable case for studying indirect transitions. From our previous knowledge[10,11] of the wave function for these states, the direct process could be expected to be somewhat hindered, and this is confirmed by the present analysis (although the direct transition came out to be stronger than predicted when using the parameters of Ref.[11]). Nevertheless, due to the collectivity of the intermediate 2^+ state in the target (and also of the transition 0^+ A $\rightarrow 2^+$ EA), the indirect transitions have a magnitude similar to the direct one. This allows the study of the interferences between the two transition amplitudes. In order to reproduce these interferences, it was necessary to use a complex effective projectile-target nucleon interaction. This effective interaction turns out to be actually almost pure imaginary, this feature being consistant with the predictions of the vibrational model. Previous evidence for an almost pure imaginary effective interaction was obtained

by Satchler[26] in a quite different way.

Several problems are yet open. First, we needed a very long range force in order to reproduce the fall off of the angular distribution. The reason is that we have mocked up the peculiar features of the higher order contributions in the effective force by using a local interaction. It has been shown [27,28] that the second order contributions such as (h,α) , (α,t) - and also (h,α) , (α,h') - are essential in explaining the main features[4,6] of the (h,t) reaction. These processes lead[27] to a strongly complex and non local effective interaction. Investigations are currently done[27] to see whether or not the long range complex interaction needed in this work arises from such processes. Also, the interference between one and two-step amplitudes depend on the phase of the optical wave functions used in the calculation. This phase seems to be independent of the particular set of parameters chosen for the optical potential. Nevertheless, it would be interesting to check the properties of the effective interaction we have observed by looking on the transitions to the 2^+ EA for other nuclei. Finally, the shift we obtain in the angular distribution should also be predicted by the vibrational model. A coupled channel analysis has been carried out[8] for these transitions, and leads to a similar shift for ^{62}Ni when a complex interaction is used. However, as said earlier, the form factor for the $G \rightarrow EA$, as well as for the $G \rightarrow A$ transition, is obtained by making the difference between the h and t optical potential, assuming isospin invariance. Part of this difference comes from the different radii of the two projectiles which are therefore absorbed at a different place. Since the change in size between the h and t particles is mainly a Coulomb effect, the assumption of these two projectiles being good analogues is not true. This cast some doubt on the origin of the imaginary part of the coupling potential in a macroscopic model of the charge exchange reaction, and was one of our motivations to undertake this study. As we have seen, one needs complex coupling even in a microscopic model. The question remains however, to see if there is a spurious part in the imaginary from factor of the macroscopic model, due to Coulomb effects. An interesting experiment would be the comparison of h and t elastic scattering on a $T=0$ nucleus at an energy high enough so that the Coulomb barrier plays a minor role. If isospin invariance holds, the h and t optical potentials should be identical, and especially it should be possible to fit the elastic cross-sections with the same radius for the imaginary potential.

One of the authors (R.S.) is grateful to the Lawrence Radiation Laboratory for its hospitality while this work was done.

REFERENCES

[1] - J.J. WESOLOWSKI, E.H. SCHWARCZ, P.G. ROOS and C.A. LUDEMANN - Phys. Rev. 169 (1968) 878 ;
L.F. HANSEN, M.L. STELTS, J.G. VIDAL and J.J. WESOLOWSKI - Phys. Rev. 174 (1968) 1155

[2] - V.A. MADSEN - Nucl. Phys. 80 (1966) 177 ;
N.K. GLENDENNING and M. VENERONI - Phys. Rev. 144 (1966) 839

[3] - G.R. SATCHLER - Nucl. Phys. A91 (1967) 1

[4] - P. KOSSANYI, P. ROUSSEL, H. FARAGGI and R. SCHAEFFER - Nucl. Phys. A148 (1970) 181

[5] - E. ROST and P.D. KUNZ - Phys. Lett. 30B (1969) 231

[6] - R. SCHAEFFER - Nucl. Phys. A164 (1971) 145

[7] - R. HINRICHS, R. SHERR, G.M. CRAWLEY and I. PROCTOR - Phys. Rev. Lett. 25 (1970) 829

[8] - P.D. KUNZ, E. ROST, R.R. JOHNSON, G.D. JONES and S.I. HAYAKAWA - Phys. Rev. 185 (1969) 1528
V.A. MADSEN et al. - Phys. Rev. Lett. 28, n°10 (1972) 629

[9] - G. BRUGE, M.S. ZISMAN, A.D. BACHER AND R. SCHAEFFER - $^{38}Ar(h,t)^{38}K$ to be published.

[10] - V. GILLET, B. GIRAUD, J. PICARD and M. RHO - Phys. Lett. 27B (1968) 483
V. GILLET, B. GIRAUD and M. RHO - private communication

[11] - R. SCHAEFFER - Nucl. Phys. A135 (1969) 231 ;
J. PICARD, O. BEER, A. EL BEHAY, P. LOPATO, Y. TERRIEN, G. VALLOIS and R. SCHAEFFER - Nucl. Phys. A128 (1969) 481

[12] - N.K. GLENDENNING - Proceedings of the International School of Physics "Enrico Fermi", Varenna (1967)

[13] - R. ASCUITTO and N.K. GLENDENNING - Phys. Rev. 181 (1969) 1396

[14] - J.C. HAFELE, E.R. FLYNN and A.G. BLAIR - Phys. Rev. 155 (1967) 1238

[15] - J.Y. PARK and G.R. SATCHLER - Particles and Nuclei, Vol.1 (1970) 233

[16] - N.K. GLENDENNING - Nucl. Phys. A117 (1968) 49

[17] - A. BOHR and B. MOTTELSON - Nucl. Structure, W.A. Benjamin, Inc. (1969) New York, Amsterdam

[18] - A. JAFFRIN and G. RIPKA - Nucl. Phys. A119 (1968) 529

[19] - R. SCHAEFFER - Thesis (1969), Rapport CEA-R-4000

[20] - R. ARVIEU - Ann. of Phys. 8 (1963) 407

[21] - E.F. GIBSON, B.W. RIDLEY, J.J. KRAUSHAAR, M.E. RICKEY, and R.H. BASSEL - Phys. Rev. 155 (1967) 1194
- E.F. GIBSON, J.J. KRAUSHAAR, B.W. RIDLEY, M.E. RICKEY and R.H. BASSEL - Phys. Rev. 155 (1967) 1208

[22] - V. GILLET and E. SANDERSON - Nucl. Phys. 54 (1964) 472

[23] - V. GILLET and M. MELKANOFF - Phys. Rev. 133 (1964) B1190

[24] - D. AGASSI and R. SCHAEFFER - Phys. Lett. 26B (1968) 703
R. SCHAEFFER - Nucl. Phys. A132 (1969) 186

[25] - R. SCHAEFFER - Proceedings of the Argonne (h,t) Symposium, Argonne, Report PHY 1970

[26] - G.R. SATCHLER - Phys. Lett.

[27] - G. BERTSCH and R. SCHAEFFER - Proceedings of the Gull Lake Symposium, Sept. 1971
- R. SCHAEFFER and G. BERTSCH - Phys. Lett. 38B, n°3 (1972) 159

[28] - A. TOYAMA - Phys. Lett. 38B, n°3 (1972) 147

TABLE CAPTIONS

Table 1 - Optical parameters for the helion and triton channels.

Table 2 - Renormalizations λ_p and λ_n of the proton and neutron densities of Gillet et al , needed in order to fit the experimental cross-section strengths. The ratio $\rho(n/p)$ of neutron to proton excitation is defined in the text.

TABLE 2

	V	r	a	W_V	r	a
h	170.6	1.143	.712	18.5	1.6	.829
t	153	1.24	.678	94.7	1.45	.841

TABLE 2

		58	60	62	64
	λ_p	4.2	3	2.6	3
	λ_n				
	pp'	1.3	0.9-1.4	1.1	
2.25 fm range	D	1.8	1.7	1.5-1.7	2
	D+I $\varphi=0$	1.7	1.5	1.3-1.5	1.7
	D+I $\varphi=\pi/4$	1.8	1.8	1.7-1.9	1.9
3 fm range	D+I $\varphi=0$	1.8	1.7	1.4-1.7	1.9
	D+I $\varphi=\pi/4$	1.9	1.7	1.6-2	2.3
	D+I $\varphi=\pi/2$	1.9	2.	1.6-1.9	2.4
$\rho(n/p)$	Th	2.8	2.6	.3	2.5
	pp'	0.9	0.8-1.2	1.3	
	D	1.2	1.4	1.7-2	1.7
	2.25 fm range D+I $\varphi=\pi/4$	1.2	1.5	1.8-2.3	1.6
	3 fm range D+I $\varphi=\pi/2$	1.3	1.7	1.8-2.2	2.

FIGURE CAPTIONS

Figure 1 - Various transitions considered in the calculations. G stands for ground state, E for excited state, A and AE for analogue and excited ananalogue states.

Figure 2 - Cross-sections for exciting the lowest 2^+ state (E) of ^{58}Ni and its analogue (AE) in ^{58}Cu. The various curves correspond to various renormalizations of the transition densities. The proton transition density is obtained from the EM transition rate, whereas the neutron transition density is adjusted

i) to reproduce the (p,p') cross-sections (dashed line), or

ii) to reproduce the (h,t) cross-section (full line, and dash-dotted line, corresponding to the two possible signs of the isovector transition density)

Figure 3 - Cross-section strength at first maximum (around 25°) for exciting the lowest 2^+ state (E) of ^{58}Ni and its analogue (AE) in ^{58}Cu as a function of the neutron transition density. λ_n is the factor by which the calculated neutron transition density is renormalized. $\rho(n/p)$ is the ratio of neutron over proton excitations, as defined in the text.

Figure 4 - Cross-section for the (h,t) transition to the 2^+ STATES (EA) in the Cu isotopes, analogues of the 2^+ collective states in Ni. The dashed line corresponds to a pure direct (D) transition, the full line to the calculation (D+I) including indirect transitions via the inelastic channels. The effective force (a 2.25fm range gaussian) for the transitions is taken to be real.

Figure 5 - Same as Fig.4, except for the effective force which is multiplied by $e^{i\pi/4}$.

Figure 6 - Same as Fig.4, except for the effective force which is multiplied by $e^{i\pi/2}$.

Figure 7 - Same as Fig.4, except for the effective force which has a longer range (3fm gaussian) and a phase $e^{i\pi/4}$.

Figure 8 - Same as Fig.4, except for the effective force which has a longer range (3fm gaussian) and a phase $e^{i\pi/2}$.

0 0 0 0 3 7 0 7 5 4 0

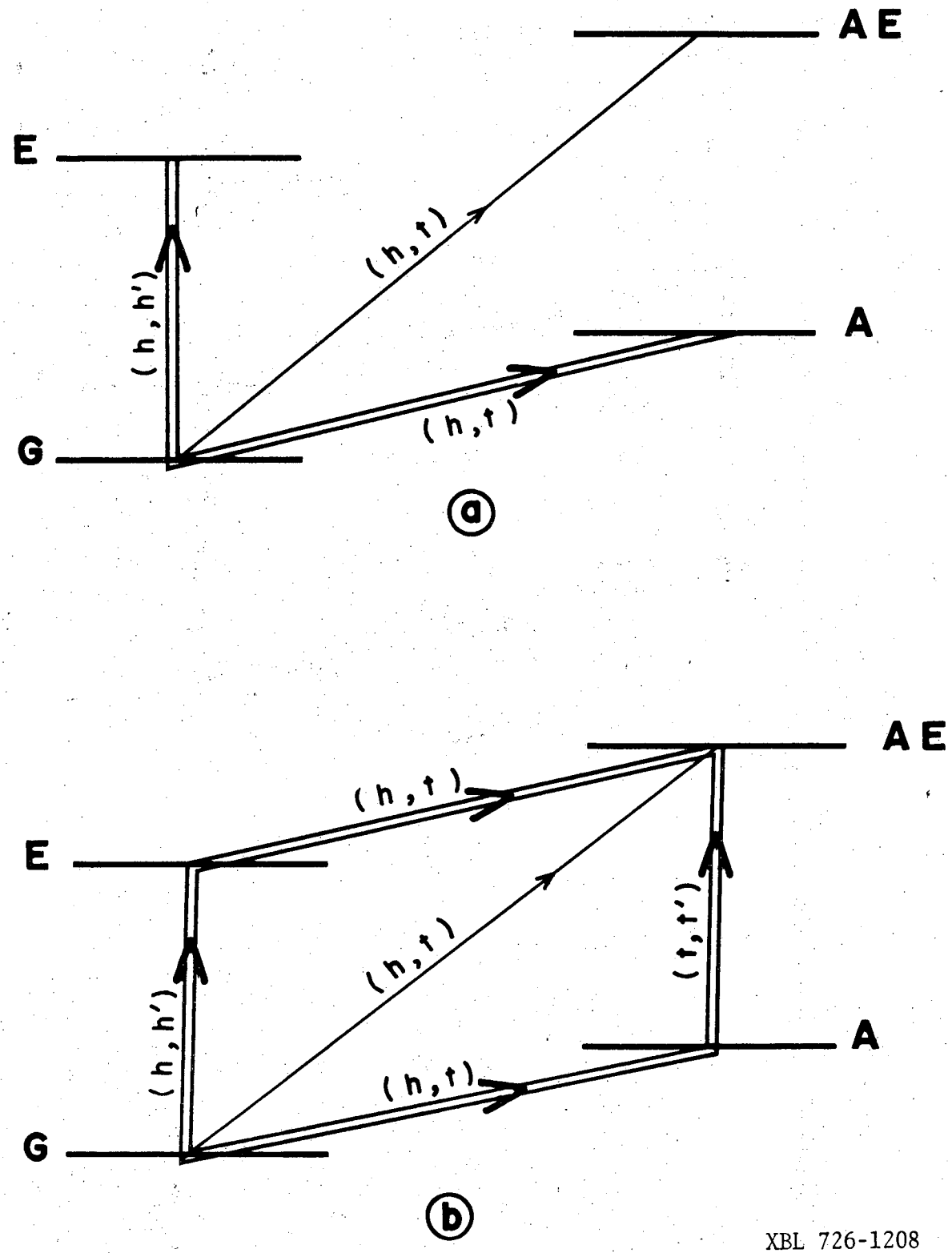

XBL 726-1208

Fig. 1

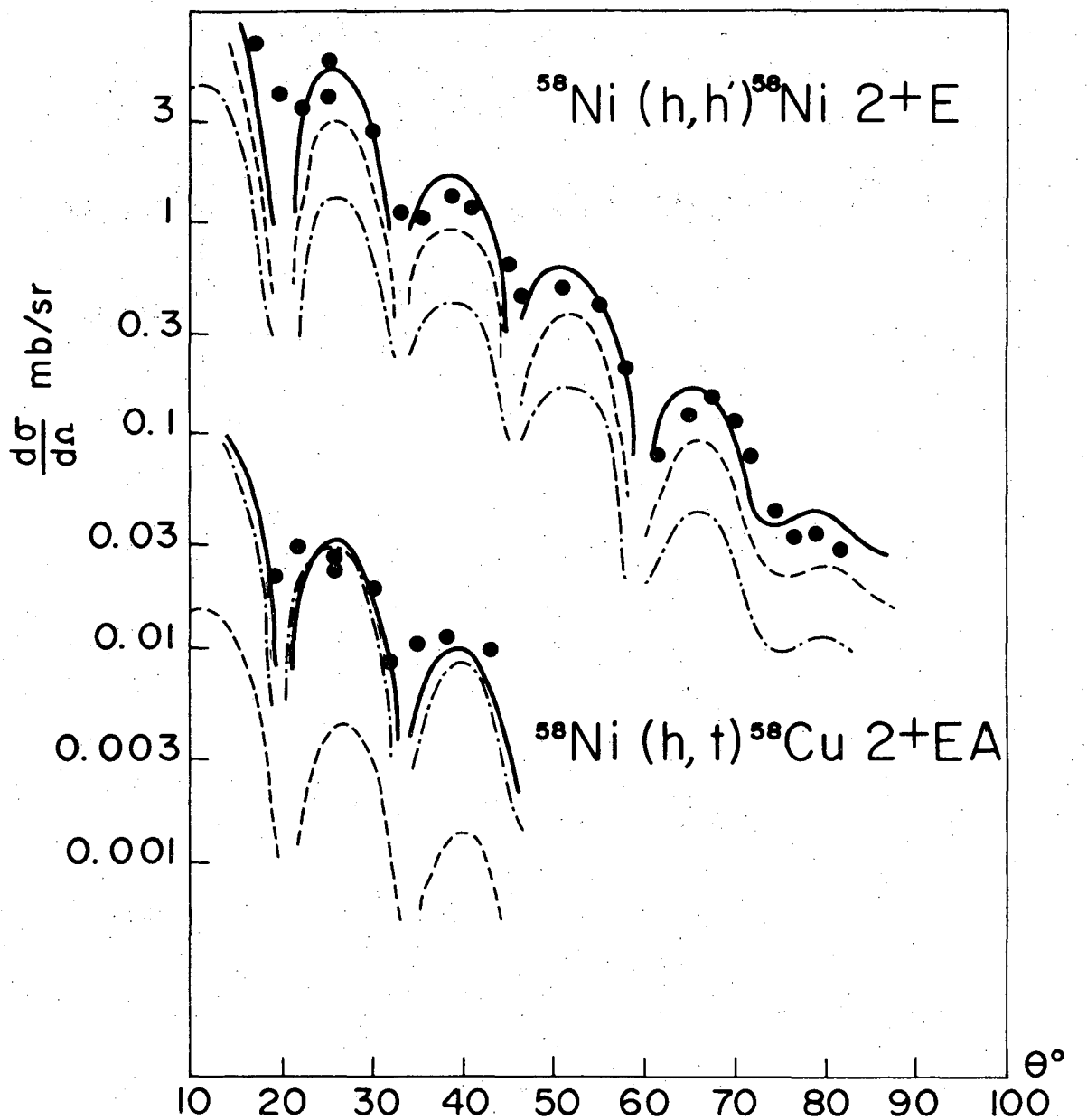

XBL 726-1209

Fig. 2

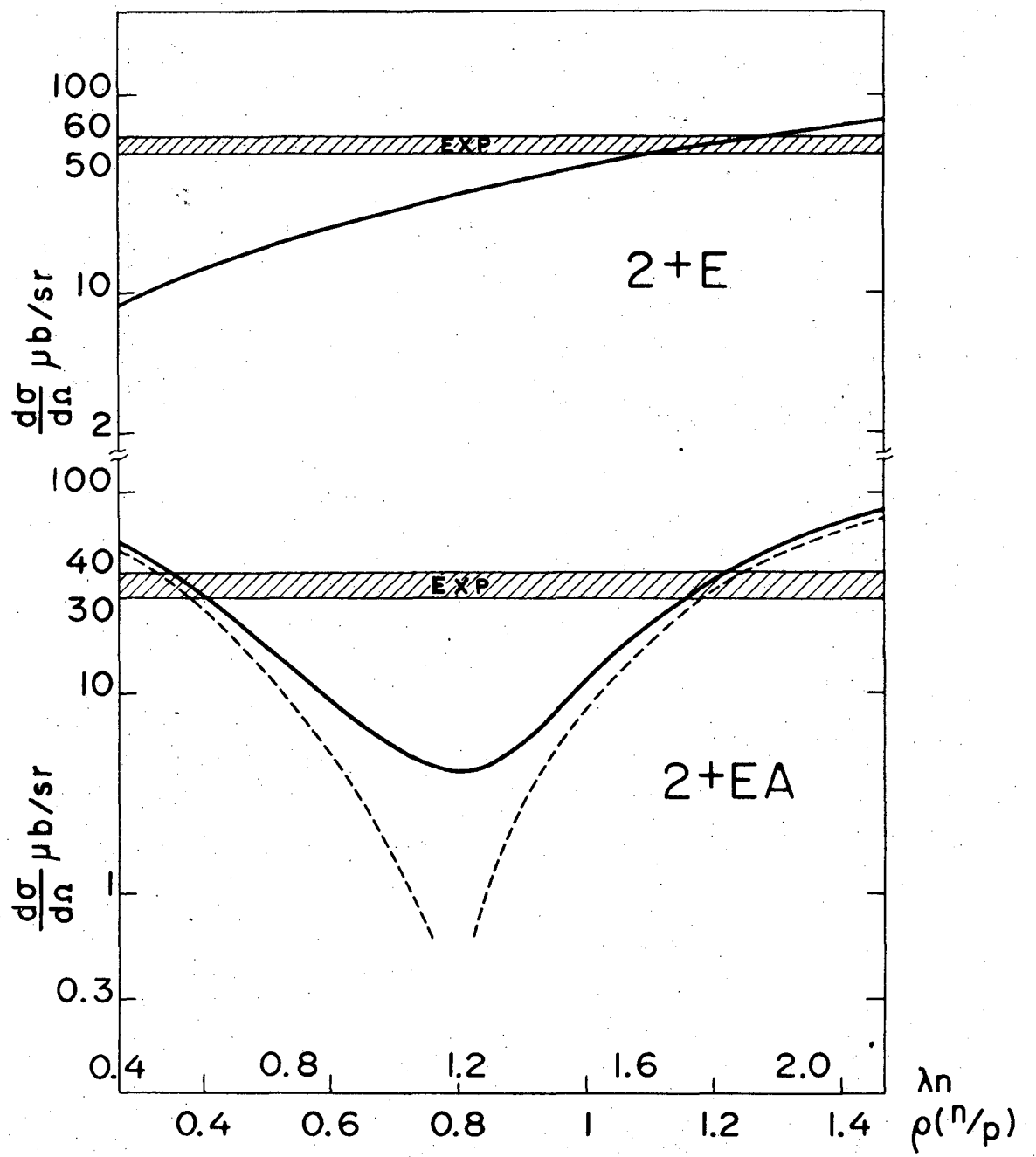

XBL 726-1210

Fig. 3

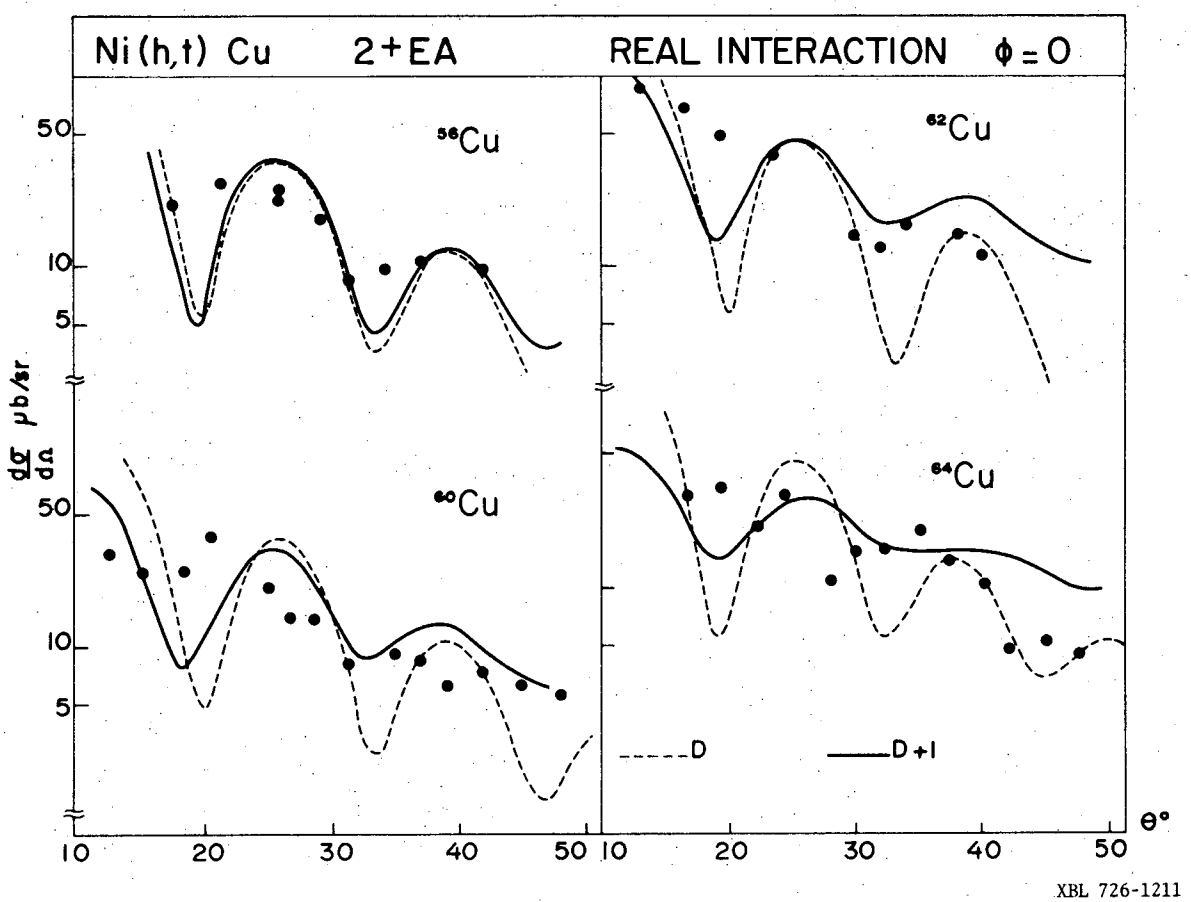
Ni(h,t) Cu 2+EA REAL INTERACTION Φ = 0
56Cu
62Cu
60Cu
64Cu
dσ/dΩ μb/sr
50
10
5
D
D+I
θ°
10
20
30
40
50
XBL 726-1211

Fig. 4

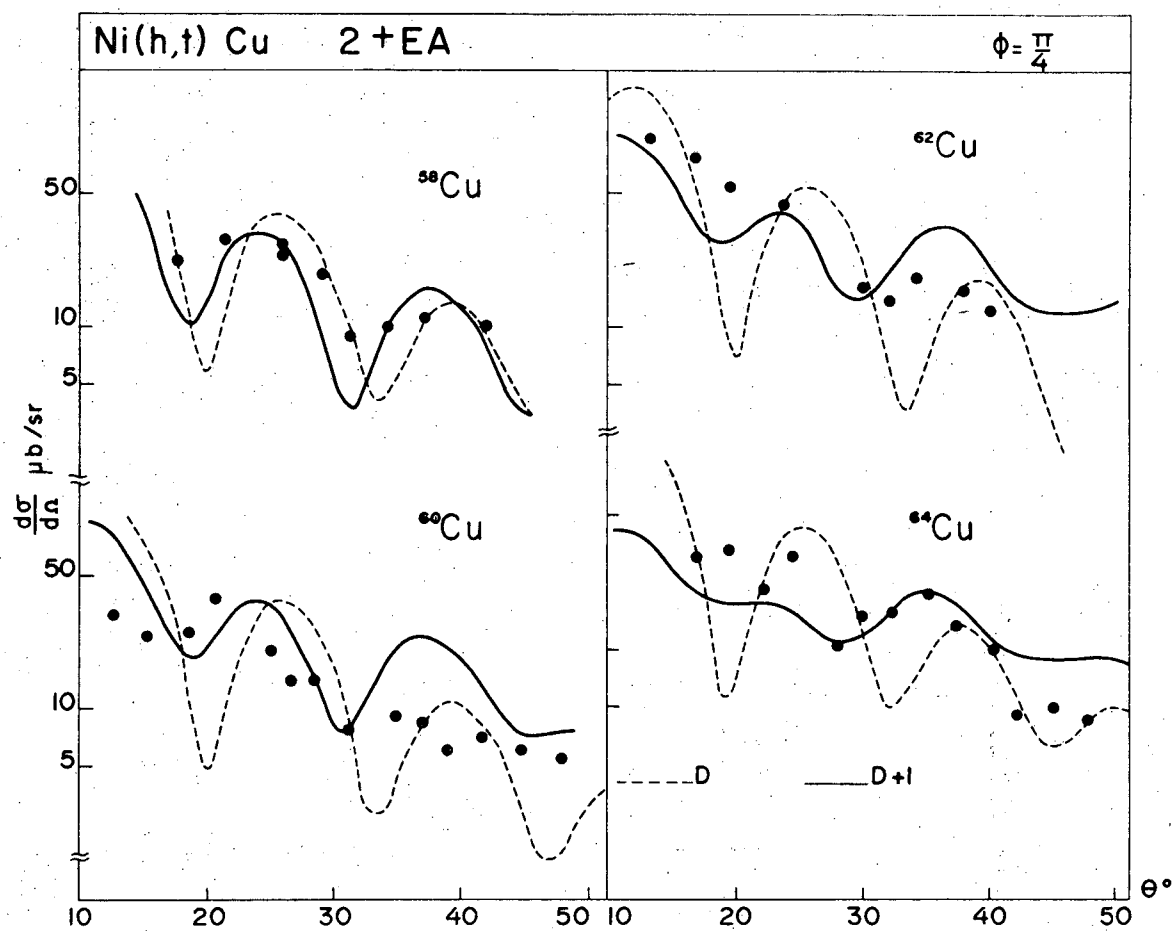

XBL 726-1212

Fig. 5

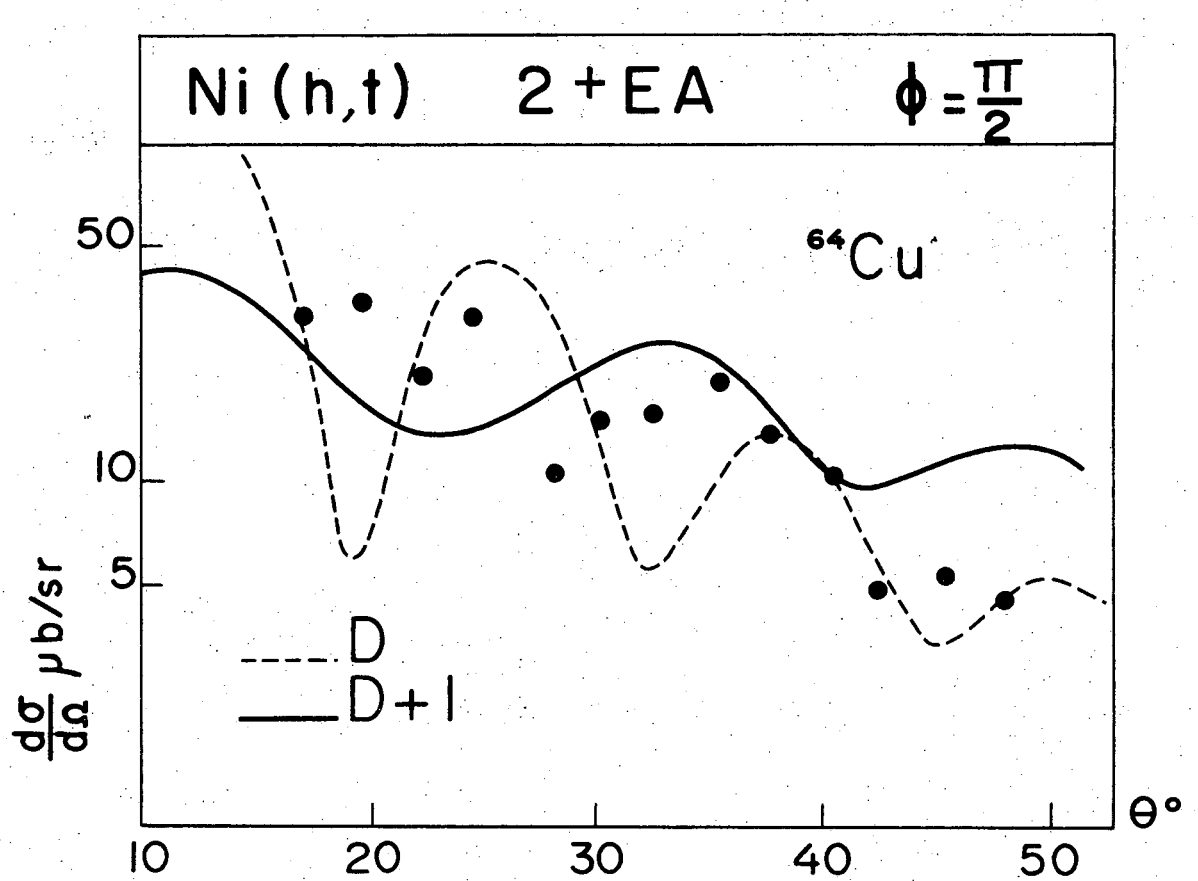

XBL 726-1213

Fig. 6

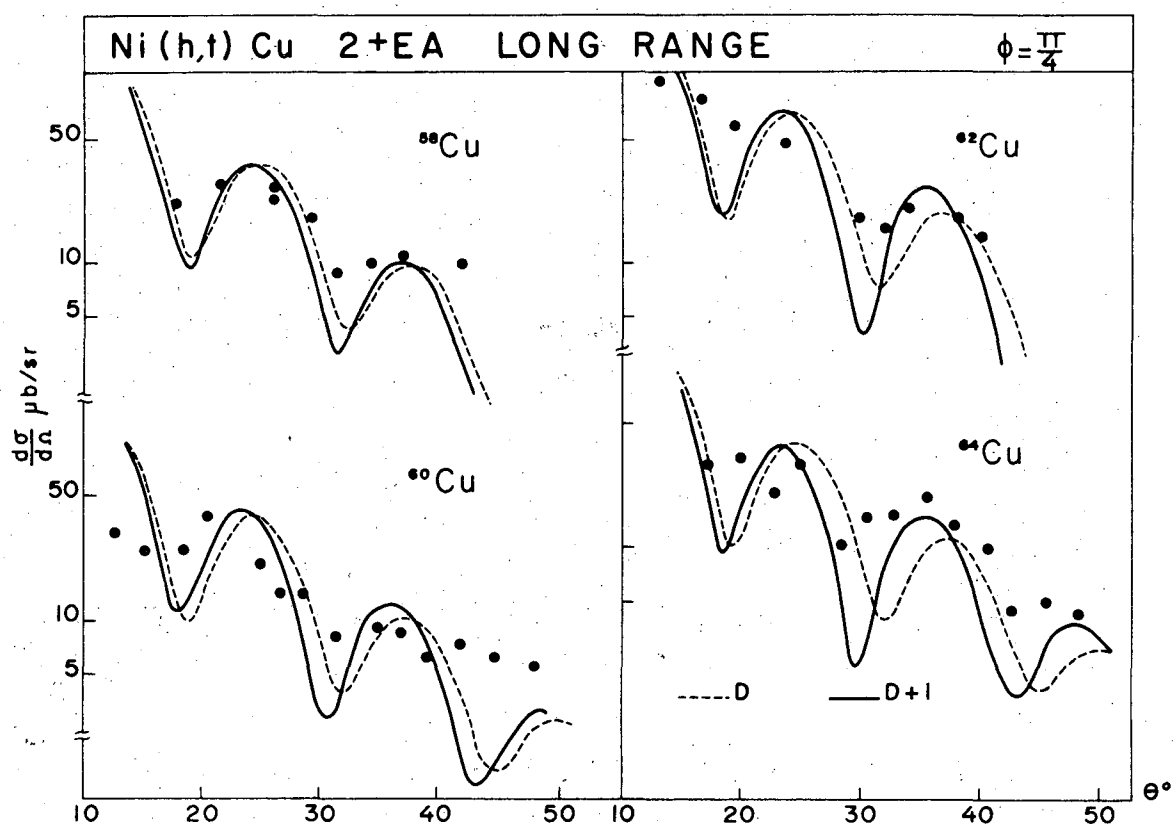

XBL 726-1214

Fig. 7

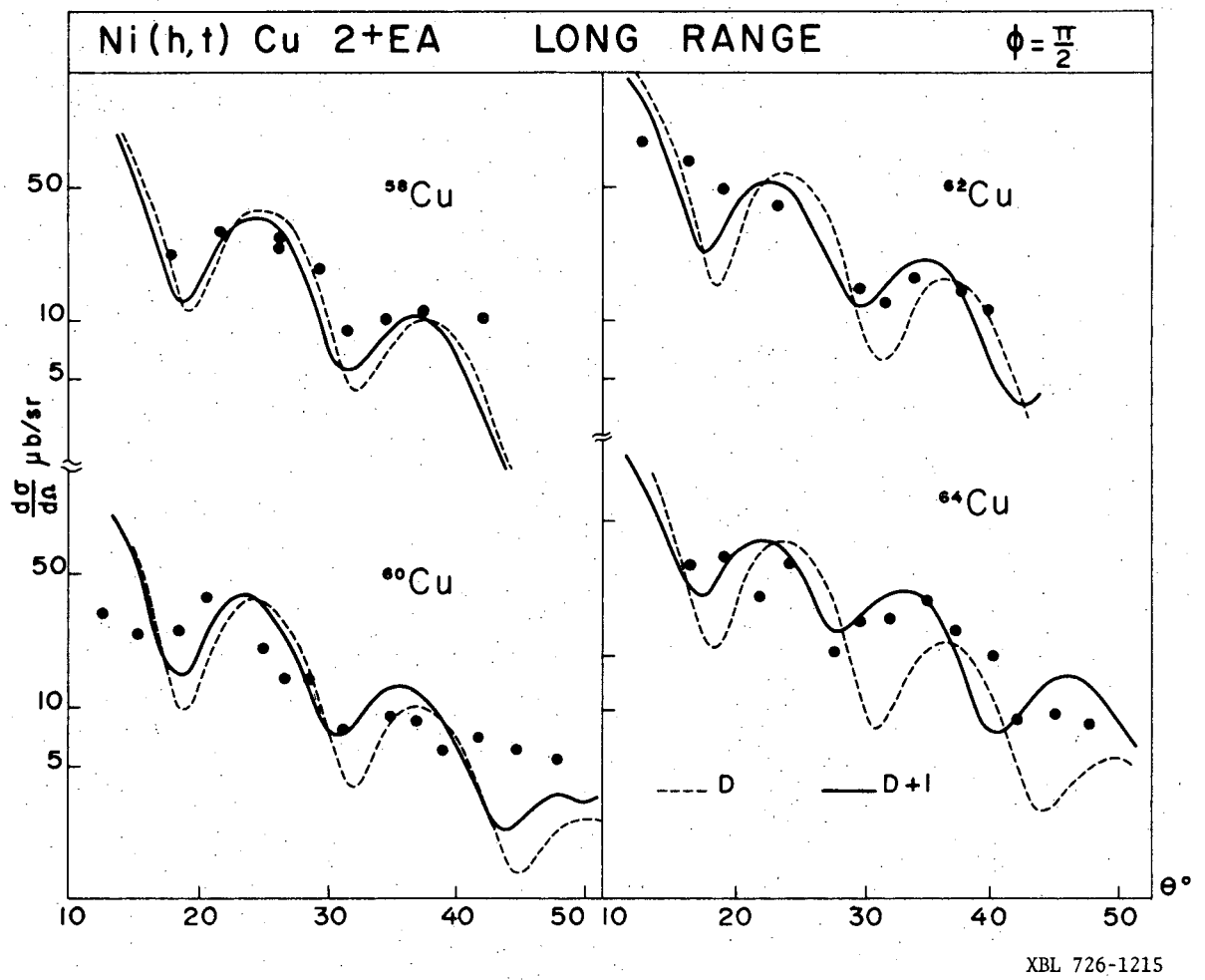
Ni(h,t) Cu 2+EA LONG RANGE
$\phi = \frac{\pi}{2}$
^{58}Cu
^{62}Cu
^{60}Cu
^{64}Cu
$\frac{d\sigma}{d\Omega}$ μb/sr
50
10
5
D
D+I
θ°
10
20
30
40
50
XBL 726-1215

Fig. 8

LEGAL NOTICE

This report was prepared as an account of work sponsored by the United States Government. Neither the United States nor the United States Atomic Energy Commission, nor any of their employees, nor any of their contractors, subcontractors, or their employees, makes any warranty, express or implied, or assumes any legal liability or responsibility for the accuracy, completeness or usefulness of any information, apparatus, product or process disclosed, or represents that its use would not infringe privately owned rights.

TECHNICAL INFORMATION DIVISION
LAWRENCE BERKELEY LABORATORY
UNIVERSITY OF CALIFORNIA
BERKELEY, CALIFORNIA 94720